Cite this article as: Yu JI, Kim JS, Park HC, Lim DH, Han YY, Lim HC, et al. Evaluation of anatomical landmark position differences between respiration-gated MRI and four-dimensional CT for radiation therapy in patients with hepatocellular carcinoma. Br J Radiol 2013;86:20120221.

Evaluation of anatomical landmark position differences between respiration-gated MRI and four-dimensional CT for radiation therapy in patients with hepatocellular carcinoma

[1]J I YU, MD, [1]J S KIM, PhD, [1]H C PARK, MD, PhD, [1]D H LIM, MD, PhD, [1]Y Y HAN, PhD, [2]H C LIM, MD, PhD and [3]S W PAIK, MD, PhD

[1]*Department of Radiation Oncology, Samsung Medical Center, Sungkyunkwan University School of Medicine, Seoul, Republic of Korea,* [2]*Department of Radiology, Samsung Medical Center, Sungkyunkwan University School of Medicine, Seoul, Republic of Korea, and* [3]*Department of Medicine, Samsung Medical Center, Sungkyunkwan University School of Medicine, Seoul, Republic of Korea*

Objective: To measure the accuracy of position differences in anatomical landmarks in gated MRI and four-dimensional CT (4D-CT) fusion planning for radiation therapy in patients with hepatocellular carcinoma (HCC).
Methods: From April to December 2009, gated MR and planning 4D-CT images were obtained from 53 inoperable HCC patients accrued to this study. Gated MRI and planning 4D-CT were conducted on the same day. Manual image fusions were performed by matching the vertebral bodies. Liver volumes and three specific anatomical landmarks (portal vein conjunction, superior mesenteric artery bifurcation, and other noticeable points) were contoured from each modality. The points chosen nearest the centre of the four landmark points were compared to measure the accuracy of fusion.
Results: The average distance differences ($\pm$standard deviation) of four validation points were 5.1 mm ($\pm$4.6 mm), 5.6 mm ($\pm$6.2 mm), 5.4 mm ($\pm$4.5 mm) and 5.1 mm ($\pm$4.8 mm). Patients who had ascites or pulmonary disease showed larger discrepancies. MRI–CT fusion discrepancy was significantly correlated with positive radiation response ($p<0.05$).
Conclusions: Approximately 5-mm anatomical landmark positional differences in all directions were found between gated MRI and 4D-CT fusion planning for HCC patients; the gap was larger in patients with ascites or pulmonary disease.
Advances in knowledge: There were discrepancies of approximately 5 mm in gated MRI–CT fusion planning for HCC patients.

Received 24 April 2012
Revised 27 July 2012
Accepted 4 September 2012

DOI: 10.1259/bjr.20120221

Many studies have reported that the treatment response and survival of hepatocellular carcinoma (HCC) patients are related to the delivered radiation dose [1–3]. Recently, detailed information on HCC and liver motion gained from the use of advanced techniques, such as a fiducial marker combined with four-dimensional (4D) planning CT, has enabled the delivery of higher doses of radiation therapy (RT) with reduced normal liver toxicity [3–5].

Although triphasic CT can provide much information about HCC, the lesion/liver contrast is higher in MRI than in CT [6, 7]. To take advantage of these benefits, there have been many efforts to incorporate liver MRI in the RT planning process [8, 9]. Moreover, several groups have demonstrated the feasibility of using cine-MRI and 4D-MRI to measure liver tumour motion for RT planning [10–12]. However, a consensus has not yet been reached on the best strategies to compensate for liver motion and adapt RT planning and delivery using planning 4D-CT combined with liver MRI.

The primary goal of this prospective study was to evaluate the accuracy of gated MRI and 4D-CT fusion planning by measuring the discrepancies in the specific anatomical landmark points of the liver between exhale-phase images of gated liver MRI and 4D-CT. We also evaluated possible factors affecting gated liver MRI and 4D-CT fusion discrepancy and RT response.

Materials and methods

Eligibility

This study investigated the accuracy of gated liver MRI and 4D-CT fusion planning for RT in patients with HCC. The eligibility criteria were a diagnosis of HCC based on the guidelines proposed by the Korea Liver Cancer Study Group, no contraindications for MRI, unresectable liver cancer, Child–Pugh classification A

Address correspondence to: Associate Professor Hee Chul Park, Department of Radiation Oncology, Samsung Medical Center, Sungkyunkwan University School of Medicine, 50 Irwon-dong, Gangnam-gu, Seoul 135-710, Republic of Korea. E-mail: rophc@skku.edu
This research was supported by the Basic Science Research Program through the National Research Foundation of Korea and funded by the Ministry of Education, Science, and Technology (2011-0004444) and IN-SUNG Foundation for Medical Research.

or B, and a life expectancy above 12 weeks. Informed consent was obtained from all patients.

Simulation

Before simulation, patients were educated and trained to control their respiration regularly and reproducibly during the whole simulation and treatment process. Patients wore video goggles during training to monitor the amplitude of their respiration with audio coaching to control their breathing constantly. The active breath-control method was not used in the 4D-CT simulation and treatment process.

On the simulation day (usually 1–2 days after training), all patients underwent 4D-CT scans in a supine position with both arms raised. Conventional skin marking and tattooing was carried out. CT images were acquired using a GE Light Speed plus 16 scanner® (General Electric, Milwaukee, WI). After free-breathing non-contrast CT images for dose calculation were obtained, intravenous contrast medium (Visapaque 270®; Amersham Health, Amersham, UK; 2 ml kg^{-1} to a maximum of 200 ml) was delivered at a rate of 5 ml s^{-1}, and exhale breath-hold CT scans were repeated at intervals of 25–30 s (arterial phase) and 50–60 s after injection (portal phase). After that, 4D-CT scans were acquired by a retrospective 4D-CT scanning technique with visual prompting goggle and Real-time Position Management systems® (RPM) (Varian Medical Systems, Palo Alto, CA). The triphasic CT and 4D-CT images were reconstructed separately with a 2.5-mm slice thickness using an Advantage Workstation® (General Electric).

Gated MR scanning without the visual prompting goggle system was conducted on the same day as the planning CT. All MRI acquisitions were performed on a Philips 3.0-T Achieva MR system® (Philips Medical Systems, Best, Netherlands). Before image acquisition, patients were placed in a supine position on a flat couch top and matched with a laser as exactly as possible. T_1 weighted non-contrast images and T_1 weighted triphasic MR images were obtained with dynamic intravenous contrast medium (Gadovist®; Schering AG, Berlin, Germany; 0.1 ml kg^{-1}), which was delivered at a rate of 2 ml s^{-1} (begun at 15–20 s for arterial enhancement, 45–50 s for portal enhancement, and delayed at 120–125 s after injection). In addition, respiration-triggered T_2 weighted single-shot fast spin-echo images at 50% of the phase (exhale phase) were also acquired with the belt-type respiratory monitoring system of the Philips MR machine. The exhale-phase gated MR images were reconstructed with a 5.0-mm slice thickness.

Gated liver MRI and four-dimensional CT fusion and accuracy measurements

To increase the accuracy of 4D-CT and gated MRI fusion planning, 4D-CT and gated MRI were registered using automated rigid image registration tools provided by our treatment planning system (Pinnacle ADAC® v. 8.0; Philips Radiation Oncology Systems, Milpitas, CA). In addition, image fusion of each exhale-phase image was performed manually using the vertebral bodies as a matching landmark by a single observer with two radiation oncologists and a physicist confirming the match. Exact liver structures were contoured for each modality according to full expiratory-phase images. Three specific anatomical landmarks were also contoured for both CT and MRI to check the accuracy of fusion planning. Anatomical landmarks were the portal vein (PV) conjunction, superior mesenteric artery (SMA) bifurcation and other noticeable points in both images. Despite the fact that the tumour itself might ultimately be the most important landmark in RT planning, we chose four anatomical structures for which the appearance on CT and MRI is such that intra- and interobserver variability would be minimised. The points chosen nearest the centre of the four landmarks were identified on each image by a radiation oncologist experienced in treating liver cancer to allow for quantitative analysis of the accuracy using our treatment planning system (Figure 1). The accuracy of the image fusion was measured by the difference in the position of pairs of all validation points. The vector value between the points on the CT and MRI was calculated as:

$$V_{SUM} = \sqrt{x^2 + y^2 + z^2}$$

where x is the left to right distance; y is the cranial to caudal distance and z is the anterior to posterior distance.

Radiation therapy

The gross tumour volumes (GTVs) were defined as the radiographically abnormal areas noted on the CT and MRI. GTV was delineated on all phases of the 4D-CT. Triphasic CT images, nearby lipiodolised lesions and anatomical landmarks were referenced in this process. We also checked the GTV in the full exhale CT and MR fusion images, but it was used only as a reference.

A 7-mm margin around the GTV within the liver and non-enhancing thromboses was included within the clinical target volume (CTV). The planning target volume (PTV) was chosen by summing all phases of the CTVs with an additional 5-mm set-up margin. Conformal planning was done with a 5-mm block margin from the PTV using three or four coplanar or non-coplanar beams of 6–10 MV X-ray. Intensity-modulated RT was not allowed. The normal liver, kidneys, stomach, duodenum and spinal cord were contoured. A dose–volume histogram (DVH) was also generated.

The radiation dose was escalated in four strata designed under tentative guidelines. Total radiation dose was determined according to the percentage of the normal liver volume irradiated at >50% of the prescribed dose. If <20% of the normal liver volume would be exposed to >50% of the prescribed dose, a total dose of 5 Gy daily for 10 fractions was selected. A dose of 4.5 Gy, 4.0 Gy or 3.5 Gy for 10 fractions was chosen when 20–35%, 35–50% or 50–75% of the liver was irradiated, respectively. In exceptional cases where full dose exposure to the stomach or duodenum was inevitable, a daily dose of 3.0 Gy for 11 fractions was prescribed to avoid gastro-duodenal toxicity.

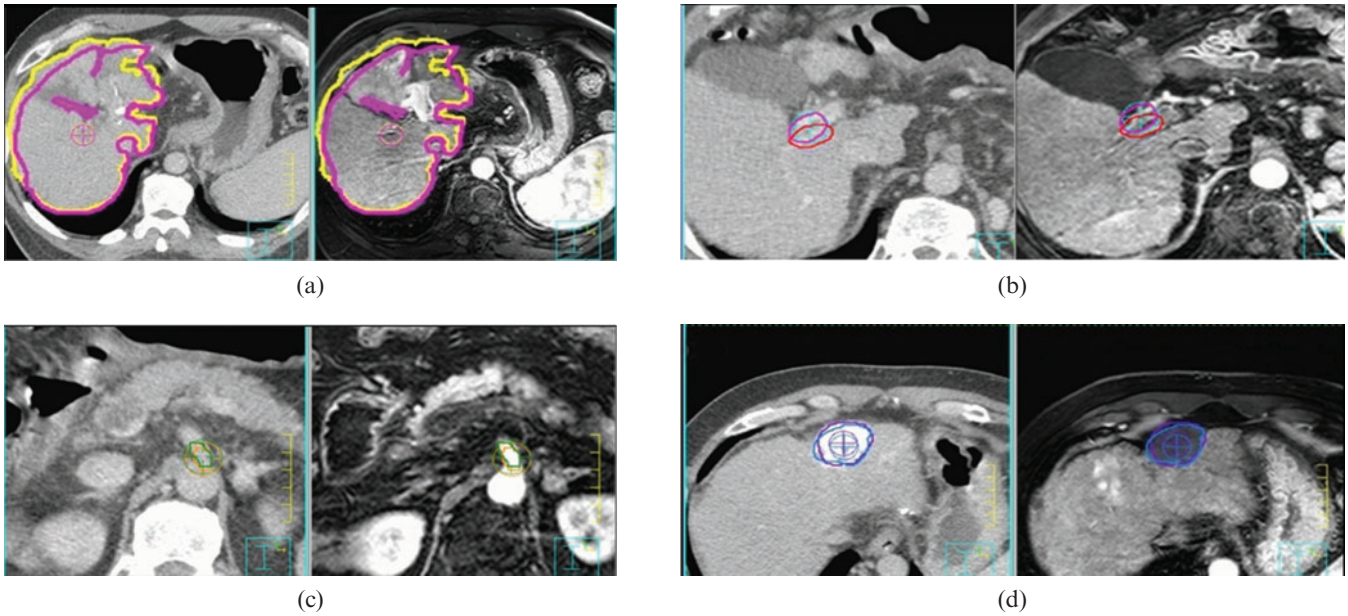

Figure 1. (a) Point chosen nearest the centre of the liver structure and (b–d) three anatomical landmarks were placed on CT and MRI fusion images. (b) Portal vein conjunction, (c) superior mesenteric artery bifurcation and (d) noticeable point.

All patients were treated with a linear accelerator equipped with an On–Board Imager® (Varian Medical Systems). In order to verify the target position, exhale-phase gated onboard imaging (OBI) was obtained daily before each treatment and compared with dynamic reconstruction and rendering (DRR) images reconstructed with 50% phase CT images from the treatment planning system. Liver dome or intrahepatic dense lipiodol deposits were compared as fiducials. In case of shifts >5 mm in fiducial positions, which was considered to be a critical margin, the OBI was retaken and the target position was verified again. When the same shift was detected, automatic adjustment for the patient's couch position was performed by the linear accelerator machine. However, gated treatment was not used in this study.

Follow-up

Patients were followed up at 1 month after completing treatment, and at intervals of 2–3 months thereafter. The treatment response was assessed using CT scans 1 month after completing RT using the response evaluation criteria in solid tumors (RECIST). During the follow-up, radiologists preferentially used lesions seen only on MRI for target lesion RECIST measurements. The objective response rate was calculated as the sum of the rate of complete response (CR) or partial response (PR).

Statistical analysis

The χ^2 test and Fisher's exact test were used to examine the relationship between the various factors and MRI–CT fusion discrepancy, and RT response. A p-value of $p<0.05$ was considered statistically significant. All calculations were performed with PASW® v. 17.0 for Windows (SPSS, Chicago, IL).

Results

Patient characteristics

Between April and December of 2009, 55 patients with HCC who had not undergone MRI during the previous month visited our department. One patient had failed to undergo MRI scanning owing to claustrophobia, and one patient did not receive RT simulation because of treatment for septic arthritis in the knee. The remaining 53 patients were analysed in this study. Because our institution generally follows guidelines proposed by the Korea Liver Cancer Study Group, there were many cases of large tumour (>10 cm diameter) treated with multiple other modalities before RT consultation. Transarterial chemo-embolisation was undertaken in all 53 patients, surgery in 9 patients (17.0%), radiofrequency ablation in 18 patients (34.0%) and prior RT in 4 patients (7.5%). In the patients who had been treated with RT before, RT dose modification was not conducted because there was an interval of more than 6 months. Detailed patient characteristics are summarised in Table 1. The median follow-up duration was 7 months.

Results of liver MRI

In 42 patients, CT and MRI provided the same information on HCC, and this information did not differ from previous data on these patients. However, MRI showed a clearer lesion–liver contrast in almost all cases (Figure 2).

New lesions, which had not been seen in the previous liver images (usually CT), were detected in 11 patients by liver MRI. For two of these patients (3.8%), all new lesions were also found on planning CT images, and in another two patients some of the new lesions were visible. In the other seven patients (13.2%), new lesions were not detected by CT. 4 of these 11 patients (7.5%)

Table 1. Patient and tumour characteristics

Variables	Number of patients (%)
Sex	
Male	47 (88.7)
Female	6 (11.3)
ECOG performance status	
0–1	46 (86.8)
2	7 (13.2)
Child–Pugh class	
A	43 (81.1)
B–C	10 (18.9)
AFP	
<400	38 (71.7)
≥400	15 (28.3)
Tumour size	
<10 cm	41 (77.4)
≥10 cm	12 (22.6)
LN metastasis	
Positive	8 (15.1)
Negative	45 (84.9)
Distant metastasis	
Positive	7 (13.2)
Negative	46 (86.8)
Ascites	
Positive	12 (22.6)
Negative	41 (77.4)
Pulmonary disease	
Positive	8 (15.1)
Negative	45 (84.9)

AFP, alpha-fetoprotein; ECOG, Eastern Cooperative Oncology Group; LN, lymph node.

showed another solitary nodule, which was included with the primary lesion in the RT target volume. The other seven patients (13.2%) received alternative treatments (usually sorafenib), starting immediately in six patients (11.3%). One patient (1.9%) received palliative RT for only the main mass and its major vascular invasion.

Accuracy of gated liver MRI and four-dimensional CT fusion planning

With rigid image registration using vertebral bodies, the average difference of the liver volume was 26.99 ml ($\pm$33.14 ml; range 0.69–161.08 ml). The difference in the point chosen nearest the centre of the liver structures and three landmarks are summarised in Table 2. In most cases, the craniocaudal distance showed the largest difference, as expected. The average vectors of displacement of the centres were 5.1–5.6 mm, which was slightly larger than the MRI slice thickness (5 mm).

Factors associated with gated liver MRI and four-dimensional CT fusion discrepancy

We used the largest vector value among the four landmarks in the statistical analysis to determine the correlation between the gated liver MRI and 4D-CT fusion discrepancy and other parameters. The cut-off point was 5 mm because it is similar to the median value of the average vectors of displacement and our institutional acceptable range.

Table 3 shows the profile of the relationship between fusion discrepancy and various parameters. A large percentage (87.5%) of patients who had pulmonary disease at simulation (pleural effusion, atelectasis or pneumonia) showed an MRI–CT fusion discrepancy of >5 mm, compared with 46.7% of patients without pulmonary disease (marginally significant at $p=0.053$). Significant differences in fusion discrepancy were detected in patients with ascites (83.3% *vs* 43.9%, $p=0.022$). The largest difference was noted in patients with ascites and/or pulmonary disease (88.9% *vs* 34.3%, $p<0.0001$).

Treatment response and prognostic factors

In 47 patients who had received RT, about 4 weeks after the completion of RT, an objective response was observed in 29 patients (61.7%), CR in 8 patients (17.0%), PR in 21 patients (44.7%) and stable in 12 patients (25.5%).

The relationship between the objective response and various parameters was analysed (Table 4). Significant prognostic factors were found to be the alpha-fetoprotein decrement after RT ($p=0.033$) and MRI–CT fusion discrepancy ($p=0.036$).

Discussion

Traditionally, RT has had a limited role in the treatment of HCC. The main reason for the current concern about RT for HCC is low tolerance of the normal liver to irradiation [13]. However, recent developments such as three-dimensional conformal RT have the potential to accurately deliver a high dose to target tumours while sparing the normal liver from high doses of RT [3, 14, 15]. Those recent data suggest that RT may be beneficial. However, challenging problems still remain in implementing RT for HCC patients [16].

Liver motion with breathing creates challenges. It is difficult not only to delineate the target volume but also to deliver radiation. However, many recent motion management strategies have been developed to use during both RT planning and delivery. Respiratory motion training with visual coaching showed an improvement in reproducibility and stability of liver movement [17]. In the simulation process, the 4D-CT scanning technique allows the establishment of a relationship between the tumour position and the respiratory phases, enabling setting of the gating window and assessment of residual tumour motion [18]. In this study, we used those systems to make the respiratory motion predictable and reproducible during simulation. To minimise interfractional variation, full exhale-phase gated OBI was checked each day before treatment and compared with full exhale DRR images from virtual simulation.

Another challenging problem is accurate target volume delineation and the detection of new lesions before the RT. Although CT is the most commonly used imaging modality in HCC, it remains relatively insensitive for the detection of small HCC or intrahepatic metastases, especially in cirrhotic patients [6]. MRI provides higher lesion to liver contrast than CT, and

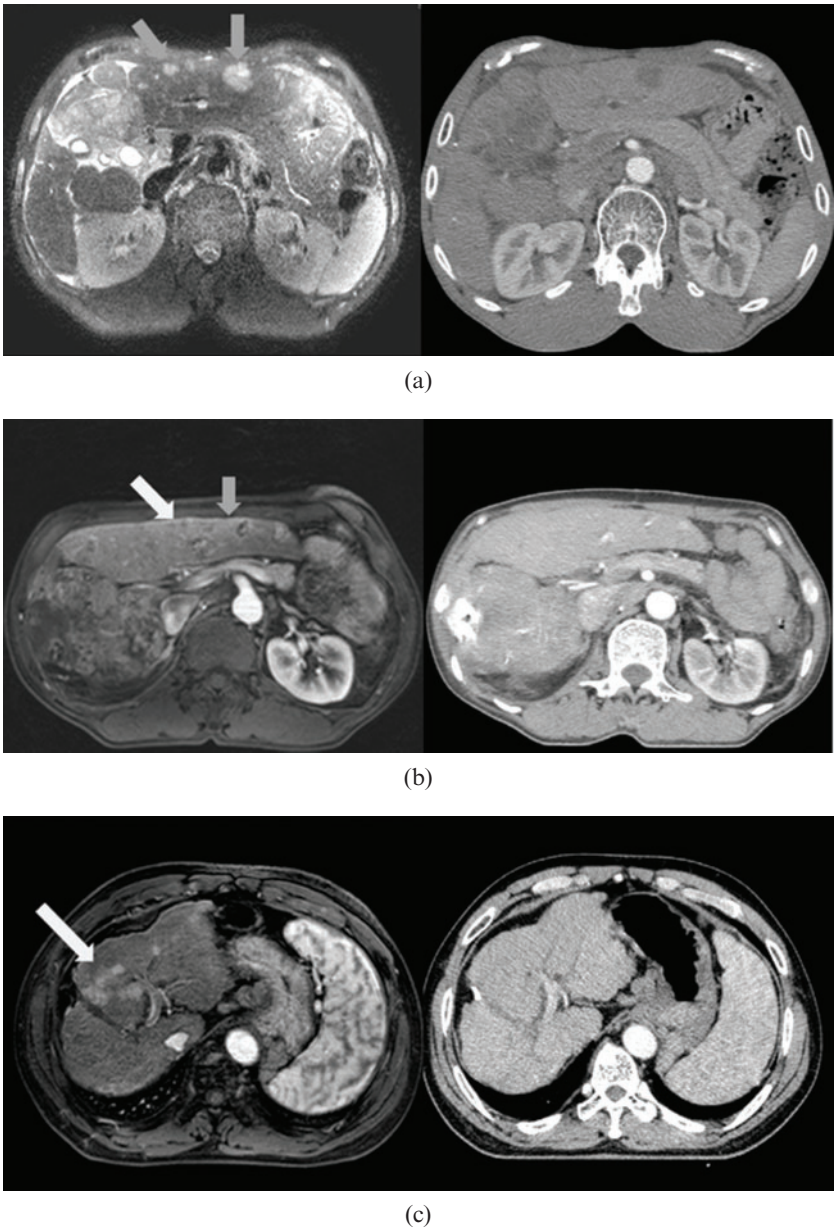

Figure 2. CT *vs* MRI comparison: MRI showed higher lesion–liver contrast. Examples show (a) visible (grey arrows), (b) partially visible (visible, grey arrow; invisible, white arrow) and (c) invisible (white arrow) groups.

new contrast agents and diffusion-weighted imaging are now being developed to increase the efficacy of tumour detection and characterisation.

There have been some attempts to use MRI for RT planning in HCC patients. Cai et al [10] reported that 4D-MRI technique with the RPM is feasible to detect liver motion. Kirilova et al [11] reported that cine-MRI can be used to facilitate individualised planning of target volume margins to account for breathing motion. Voroney et al [9] used a deformable registration tool for RT planning, and concluded that it allows for more accurate comparisons of liver and tumour volumes.

Despite these advantages of MRI, the liver motion problem presents a significant obstacle to using MRI directly in RT planning. Several deformable image registration algorithms have been suggested and actively investigated recently; however, algorithmic accuracy has been tested inconsistently, test cases are usually limited to a narrow range of clinical situations and reported errors vary widely for similar methods [19, 20].

Under the circumstances, we used a rigid registration method in fusion planning to get additional information from MRI. To verify the registration, we performed this study and checked the accuracy of fusion planning.

In this study, the differences in the point chosen nearest the centre of the liver structures and three landmarks were 5.1 mm ($\pm$4.6), 5.6 mm ($\pm$6.2), 5.4 mm ($\pm$4.5) and 5.1 mm ($\pm$4.8). Those results are quite similar to Guckenberger et al's [4] report that the 4–6-mm margin was calculated to compensate for intrafractional drifts of the liver, and slightly larger than Voroney's 3.7-mm median of the average distance between the CT tumour surface and MRI tumour surface [9].

The absolute divergence in each direction was not great in our study; the craniocaudal distance showed the largest gap, as we expected. Because CT and MR images were not collected at the same time in this study, there could be changes in organ positions between CT and MRI simulation. However, organ motion also occurs between fractions. Those discrepancies thus need to be

Table 2. Absolute distance of four validation points (centroid of the liver structure and three anatomical landmarks) between exhale CT and exhale MR images for all patients

Axis	Distance (± standard deviation) (mm)			
	Liver	Noticeable point	PV conjunction	SMA bifurcation
x (L-R)	1.7 (±2.1)	2.3 (±2.2)	1.8 (±1.9)	2.5 (±3.3)
y (C-C)	3.3 (±4.1)	3.6 (±6.1)	3.2 (±3.8)	2.1 (±2.8)
z (A-P)	2.3 (±2.6)	2.2 (±2.2)	2.8 (±3.1)	2.8 (±3.4)
V_{SUM}	5.1 (±4.6)	5.6 (±6.2)	5.4 (±4.5)	5.1 (±4.8)

A-P, anterior–posterior; C-C, craniocaudal; L-R, left–right; PV, portal vein; SMA, superior mesenteric artery; V_{SUM}, vector value between the points on CT and MR images.

considered in RT planning because the variation may occur during RT. This idea is supported by the result that patients with >5 mm fusion discrepancies showed lower response rates in our study.

As a result, 40% of all patients, and >60% of patients without ascites or pulmonary disease, showed <5-mm discrepancies of all four validation points. Based on these results, we conclude that at least 5 mm additional margin in all directions is needed to perform a gated liver MRI and 4D-CT fusion planning process, and special concern is necessary in patients with ascites or pulmonary disease.

Considering the advantages of liver MRI and the superior lesion to liver contrast ratio, gated liver MRI and 4D-CT fusion planning appears to be a good choice for HCC patients planning to undergo RT. However, patients who had ascites or pulmonary disease showed significantly higher rates of MRI–CT fusion discrepancy. As known, daily respiration of these patients could be more unstable than in other patients. This instability was directly related to the poor radiation response in our study and occurred not only during MRI–CT simulation but also during daily radiation delivery. Special consideration should be given to daily radiation delivery as well as to RT planning in patients associated with unstable respiratory motion.

Table 3. Factors associated with liver MRI–CT image fusion discrepancy >5 mm of any validation point

Variables	No. of patients	No. of patients with fusion discrepancy >5 mm (%)	*p*-value
Sex			
Male	47	24 (51.0)	0.672
Female	6	4 (66.7)	
ECOG performance			
0–1	46	24 (51.1)	0.234
≥2	7	4 (57.1)	
Child–Pugh classification			
A	43	21 (48.8)	0.172
B–C	10	7 (70.0)	
LN metastasis			
Positive	8	4 (50.0)	1.000
Negative	45	24 (53.3)	
Distant metastasis			
Positive	7	2 (28.6)	0.234
Negative	46	26 (56.5)	
Tumour size			
<10 cm	41	21 (51.2)	0.750
≥10 cm	12	7 (58.3)	
Number of tumours			
Solitary	25	14 (56.0)	0.785
Multiple	28	14 (50.0)	
Ascites			
Positive	12	10 (83.3)	0.022
Negative	39	18 (43.9)	
Pulmonary disease			
Positive	8	7 (87.5)	0.053
Negative	45	21 (46.7)	
Ascites or pulmonary disease			
Positive	18	16 (88.9)	<0.001
Negative	35	12 (34.3)	

ECOG, Eastern Cooperative Oncology Group; LN, lymph node.

To our knowledge, there are few reports on the accuracy of MRI–CT fusion planning and interfractional variation on the clinical results of RT in HCC patients. This study is therefore significant because it provided valuable information about adequate margins for both gated liver MRI and 4D-CT fusion planning and daily RT delivery. Our study also used a diagnostic MRI machine and manual matching, which might be easily accessible, and used a time-saving protocol compared with other reports about planning MRI.

We note that our study also had some limitations. Major limitations include collection of CT and MRI at separate times and fusion planning of only a single full exhale phase. Second, we used a diagnostic MRI machine and manual matching. Considering that liver motion is complex, consisting of translations, rotations and hysteresis, rigid registration may not be enough [21]. Further studies may solve those limitations of methods in MRI–CT fusion planning.

Third, to check the accuracy of fusion planning, we analysed anatomical landmarks other than the tumour itself. The tumour might well be the most important landmark in RT planning, ultimately, but, to accomplish this goal, it might be better to select specific landmarks agreeable to everybody. Therefore, we could not analyse survival results and related prognostic factors. Further large-scale prospective studies may resolve remaining questions.

In conclusion, MRI provided information on CT-invisible intrahepatic metastasis and showed much higher lesion to liver contrast than CT. In the MRI–CT fusions, patients who had ascites or pulmonary disease at simulation showed larger discrepancies. Moreover, the size of the discrepancy was related to a lower response rate to RT. MRI–CT fusion planning may be a good choice for HCC patients planning to undergo RT, but treatment delivery in patients with ascites or pulmonary disease at simulation should be chosen carefully.

Table 4. Factors associated with radiation therapy (RT) response

Variables	No of patients	No of (+) response (%)	*p*-value
Sex			
Male	41	25 (61.0)	1.000
Female	6	4 (66.7)	
ECOG performance			
0–1	41	26 (63.4)	0.662
≥2	6	3 (50.0)	
Child–Pugh class			
A	39	25 (64.1)	0.692
B–C	8	4 (50.0)	
AST			
≤80	37	27 (73.0)	0.004
>80	10	2 (20.0)	
ALT			
≤80	35	23 (65.7)	0.493
>80	12	6 (50.0)	
ALP			
≤150	37	23 (62.2)	1.000
>150	10	6 (60.0)	
RT dose (BED, $\alpha/\beta=10$)			
≥55 Gy	21	15 (71.4)	0.245
<55 Gy	26	14 (53.8)	
Pre-treatment AFP			
≥400	35	23 (65.7)	0.493
<400	13	6 (50.0)	
Tumour size			
<10 cm	35	24 (68.6)	0.095
≥10 cm	12	5 (41.7)	
Number of tumours			
Solitary	23	16 (69.6)	0.371
Multiple	24	13 (54.2)	
Ascites			
Positive	7	2 (28.6)	0.089
Negative	40	27 (67.5)	
Pulmonary disease			
Positive	3	0 (0.0)	0.050
Negative	44	29 (65.9)	
Ascites or pulmonary disease			
Positive	9	2 (22.2)	0.018
Negative	38	27 (71.1)	
AFP decrement after RT			
Positive	26	20 (76.9)	0.033
Negative	21	9 (42.9)	
CT/MRI fusion mismatch			
Positive	24	11 (45.8)	0.036
Negative	23	18 (78.3)	

AFP, alpha-fetoprotein; ALP, alkaline phosphatase; ALT, alanine aminotransferase; AST, aspate aminotransferase; BED, biologically effective dose; ECOG, Eastern Cooperative Oncology Group; LN, lymph node.

References

1. Dawson LA, Ten Haken RK. Partial volume tolerance of the liver to radiation. Semin Radiat Oncol 2005;15:279–83.
2. Lo SS, Dawson LA, Kim EY, Mayr NA, Wang JZ, Huang Z, et al. Stereotactic body radiation therapy for hepatocellular carcinoma. Discov Med 2010;9:404–10.
3. Park HC, Seong J, Han KH, Chon CY, Moon YM, Suh CO. Dose-response relationship in local radiotherapy for hepatocellular carcinoma. Int J Radiat Oncol Biol Phys 2002;54:150–5.
4. Guckenberger M, Sweeney RA, Wilbert J, Krieger T, Richter A, Baier K, et al. Image-guided radiotherapy for liver cancer using respiratory-correlated computed tomography and cone-beam computed tomography. Int J Radiat Oncol Biol Phys 2008;71:297–304.
5. Wurm RE, Gum F, Erbel S, Schlenger L, Scheffler D, Agaoglu D, et al. Image guided respiratory gated hypofractionated stereotactic body radiation therapy (H-SBRT) for liver and lung tumors: initial experience. Acta Oncol 2006;45:881–9.
6. Ariff B, Lloyd CR, Khan S, Shariff M, Thillainayagam AV, Bansi DS, et al. Imaging of liver cancer. World J Gastroenterol 2009;15:1289–300.
7. Willatt JM, Hussain HK, Adusumilli S, Marrero JA. MR imaging of hepatocellular carcinoma in the cirrhotic liver: challenges and controversies. Radiology 2008;247:311–30.
8. Pech M, Mohnike K, Wieners G, Bialek E, Dudeck O, Seidensticker M, et al. Radiotherapy of liver metastases. Comparison of target volumes and dose-volume histograms employing CT- or MRI-based treatment planning. Strahlenther Onkol 2008;184:256–61.
9. Voroney JP, Brock KK, Eccles C, Haider M, Dawson LA. Prospective comparison of computed tomography and magnetic resonance imaging for liver cancer delineation using deformable image registration. Int J Radiat Oncol Biol Phys 2006;66:780–91.
10. Cai J, Chang Z, Wang Z, Paul Segars W, Yin FF. Four-dimensional magnetic resonance imaging (4D-MRI) using image-based respiratory surrogate: a feasibility study. Med Phys 2011;38:6384–94.
11. Kirilova A, Lockwood G, Choi P, Bana N, Haider MA, Brock KK, et al. Three-dimensional motion of liver tumors using cine-magnetic resonance imaging. Int J Radiat Oncol Biol Phys 2008;71:1189–95.
12. Korin HW, Ehman RL, Riederer SJ, Felmlee JP, Grimm RC. Respiratory kinematics of the upper abdominal organs: a quantitative study. Magn Reson Med 1992;23:172–8.
13. Guha C, Kavanagh BD. Hepatic radiation toxicity: avoidance and amelioration. Semin Radiat Oncol 2011;21:256–63.
14. Gunderson LL, Haddock MG, Foo ML, Todoroki T, Nagorney D. Conformal irradiation for hepatobiliary malignancies. Ann Oncol 1999;10(Suppl. 4):221–5.
15. Mornex F, Girard N, Beziat C, Kubas A, Khodri M, Trepo C, et al. Feasibility and efficacy of high-dose three-dimensional-conformal radiotherapy in cirrhotic patients with small-size hepatocellular carcinoma non-eligible for curative therapies: mature results of the French Phase II RTF-1 trial. Int J Radiat Oncol Biol Phys 2006;66:1152–8.
16. Seong J. Challenge and hope in radiotherapy of hepatocellular carcinoma. Yonsei Med J 2009;50:601–12.
17. Korreman SS, Juhler-Nottrup T, Fredberg Persson G, Navrsted Pedersen A, Enmark M, Nystrom H, et al. The role of image guidance in respiratory gated radiotherapy. Acta Oncol 2008;47:1390–6.
18. Rietzel E, Rosenthal SJ, Gierga DP, Willet CG, Chen GT. Moving targets: detection and tracking of internal organ motion for treatment planning and patient set-up. Radiother Oncol 2004;73(Suppl. 2):S68–72.
19. Coselmon MM, Balter JM, McShan DL, Kessler ML. Mutual information based CT registration of the lung at exhale and inhale breathing states using thin-plate splines. Med Phys 2004;31:2942–8.
20. Rohlfing T, Maurer Jr CR, O'Dell WG, Zhong J. Modeling liver motion and deformation during the respiratory cycle using intensity-based nonrigid registration of gated MR images. Med Phys 2004;31:427–32.
21. Shirato H, Seppenwoolde Y, Kitamura K, Onimura R, Shimizu S. Intrafractional tumor motion: lung and liver. Semin Radiat Oncol 2004;14:10–18.